Developmental Cell, Volume *22*

Supplemental Information

Regeneration of Amputated Zebrafish Fin Rays from De Novo Osteoblasts

Sumeet Pal Singh, Jennifer E. Holdway, and Kenneth D. Poss

Inventory of Supplemental Information

Figure S1. Characterization of transgenic lines used in the paper. Supports Figure 1.

Figure S2. Provides further analysis of the inducible osteoblast ablation system. Supports and extends results of Figure 2.

Figure S3. Further characterizes the effects of osteoblast ablation on fin amputation and regeneration. Supports and extends results of Figure 3.

Figure S4. Quantifies loss of lineage-tracing label upon osteoblast ablation. Supports Figure 4.

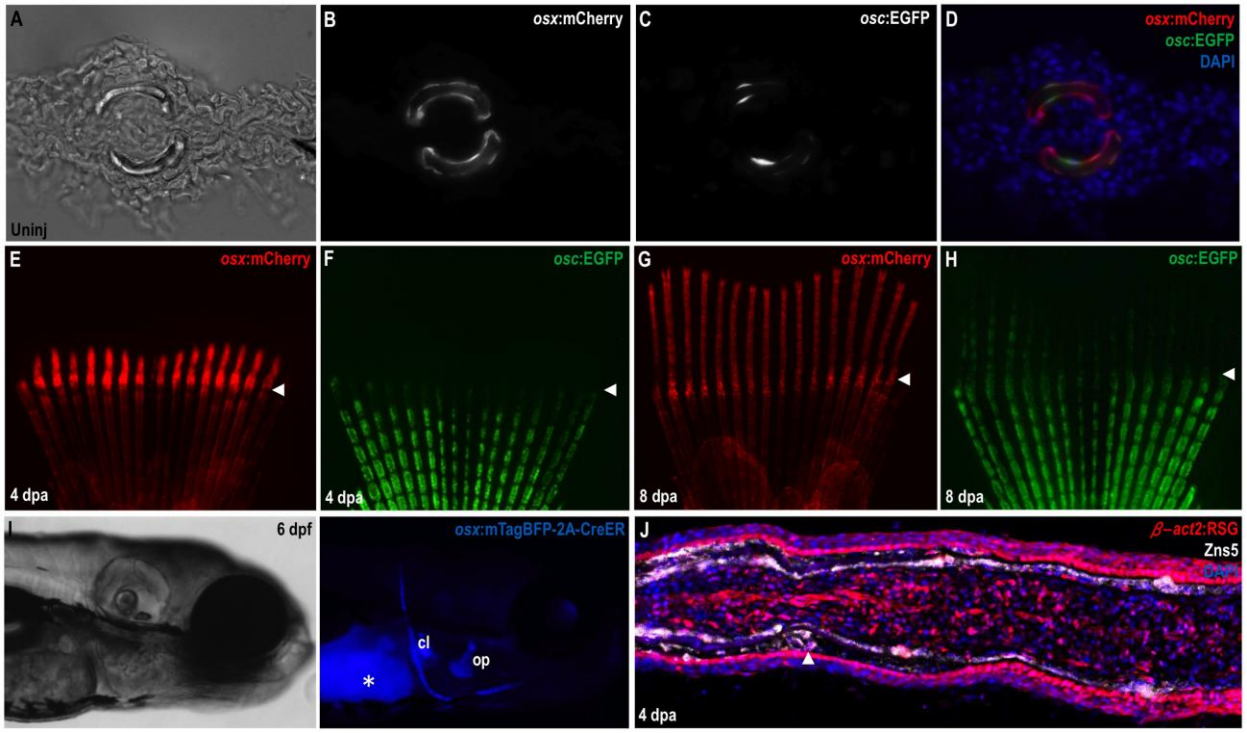

Figure S1. Osteoblast-Specific Transgenic Reporter and Lineage-Labeling Strains

(A-D) Transverse section through an uninjured caudal fin from an *osx:mCherry; osc:EGFP* double transgenic animal. Fin hemirays are outlined by *osx:*mCherry^{+} osteoblasts, most of which are also positive for *osc:*EGFP fluorescence.

(E-H) Regenerating fins of *osx:mCherry; osc:EGFP* animals shown at 4 (E, F) and 8 (G, H) dpa. *osx:*mCherry is easily visible in the regenerate by 4 dpa, while *osc:*EGFP fluorescence emerges at 7-8 dpa. Arrowheads indicate amputation planes.

(I) Bright field (left) and fluorescent (right) images of a 6 dpf *osx:CreER* larva, indicating blue mTagBFP fluorescence in bone structures. Asterisk, yolk autofluorescence. cl, clethium; op, opercule.

(J) Section through a 4 dpa *β-act2:RSG* fin regenerate. DsRed fluorescence is detectable in most cells, indicating that the line is suitable for genetic fate-mapping of fin tissues.

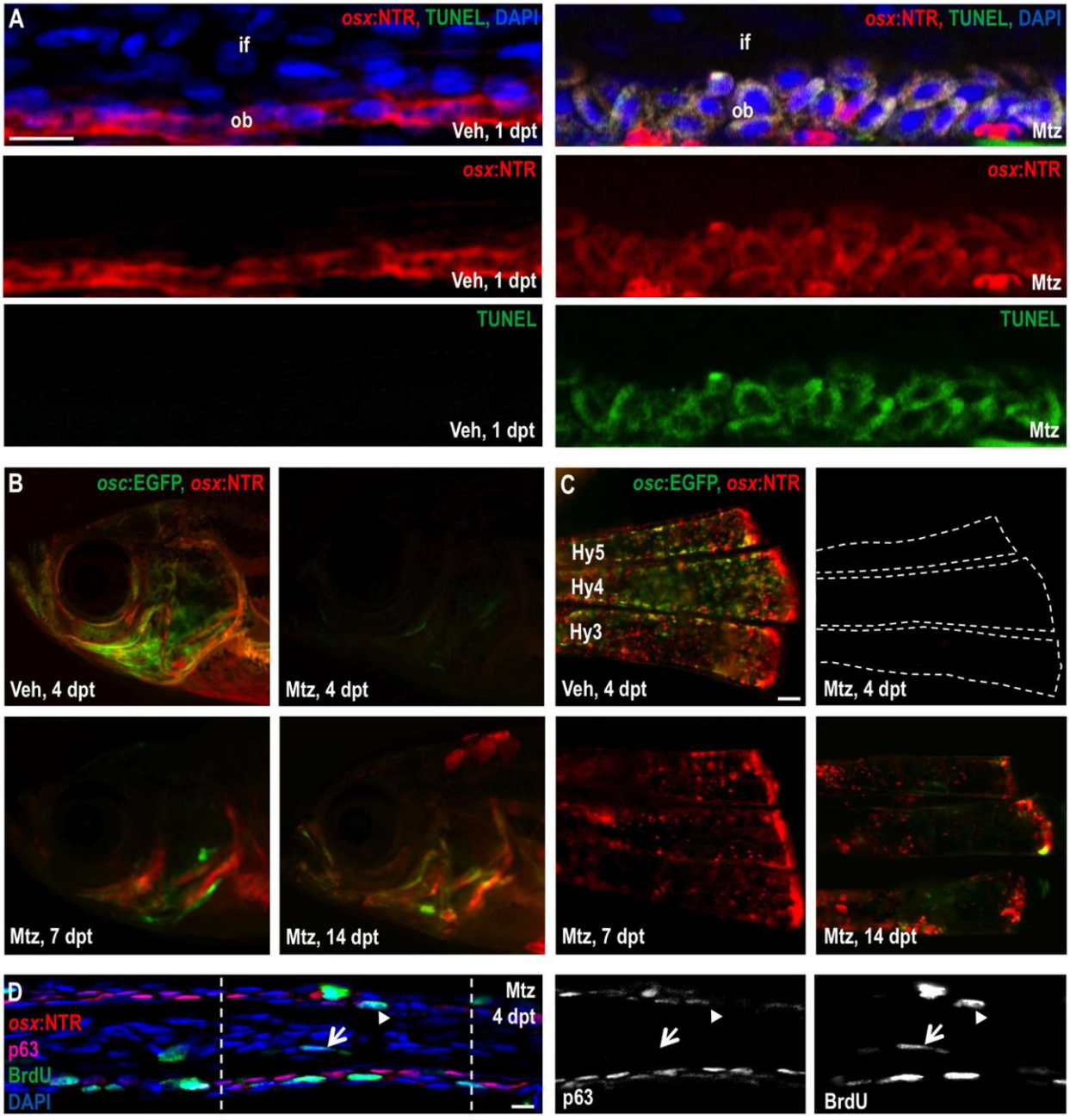
A
osx:NTR, TUNEL, DAPI
if
ob
Veh, 1 dpt
Mtz
osx:NTR
TUNEL
B
osc:EGFP, osx:NTR
Veh, 4 dpt
Mtz, 4 dpt
Mtz, 7 dpt
Mtz, 14 dpt
C
Hy5
Hy4
Hy3
D
Mtz
4 dpt
p63
BrdU
DAPI

Figure S2. Effects of Osteoblast Ablation

(A) High magnification image of TUNEL staining of *osx:NTR* fins 24 hours after vehicle (left) or Mtz (right) treatment. TUNEL signals were not detected in vehicle-treated osteoblasts, while only *osx:*NTR^{+} cells displayed TUNEL staining after Mtz treatment. Note that osteoblasts show an atypical rounded appearance 24 hours after Mtz treatment, as well as perinuclear/cytosolic TUNEL staining similar to what that reported for cardiomyocytes after diphtheria toxin A-mediated ablation (Wang et al., 2011). Scale bar = 100 µm.

(B) Cranial images of *osx:NTR; osc:EGFP* fish, showing major loss of osteoblast marker fluorescence within 4 days of Mtz treatment. Expression of *osx:*NTR is undetectable, while very low green fluorescence can be detected. Autofluorescence may be a factor due to a higher exposure time than Figure 2A. *osx:*NTR and *osc:*EGFP signals show recovery at 7 and 14 days post-treatment (dpt).

(C) Hypurals 3, 4 and 5 (Hy3-5) of adult *osx:NTR; osc:EGFP* fish were imaged after fixation and complete removal of overlying tissues. Dramatic loss of fluorescent reporters occurs by 4 days after Mtz treatment, while recovery is evident at 7 and 14 dpt.

(D) BrdU was injected into *osx:NTR* animals 4 days after Mtz treatment. Tissue is co-stained with p63 (magenta), which marks basal epidermal cells. Proliferating epidermal cells (arrowhead) and non-epidermal cells (arrow) are evident in the absence of detectable osteoblasts, indicating a diverse cellular proliferative response to the ablation.

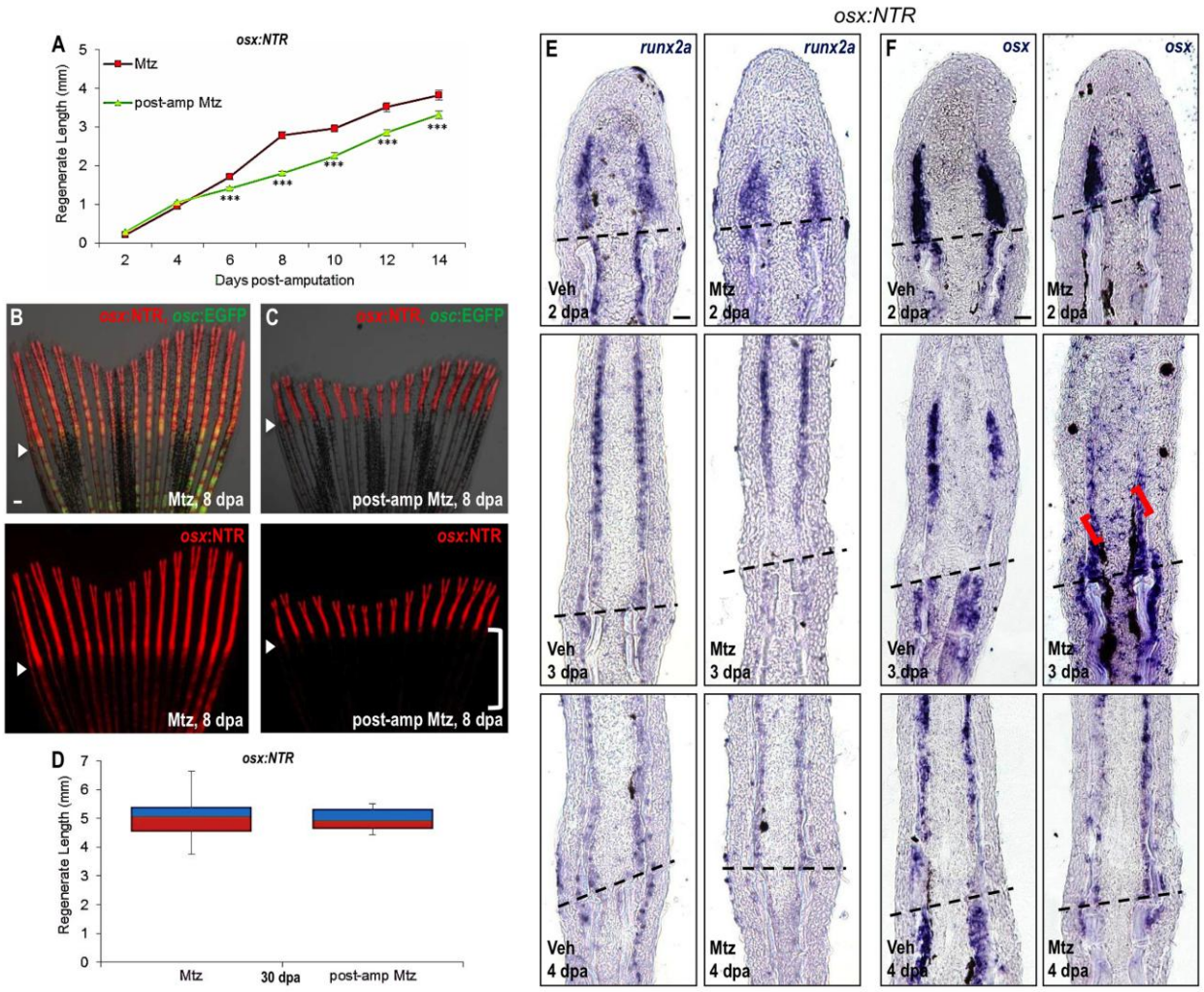

Figure S3. Induction of the Early Osteoblast Marker *runx2a* in the Regenerate after Ablation

(A) *osx:NTR* animals treated with vehicle before amputation and with Mtz 4 days after amputation (post-amp Mtz) display a slower rate of regeneration as compared to those treated with Mtz 2 days before amputation (Mtz). An additional control group, showing normal regeneration and not indicated on this graph, was wild-type animals treated with Mtz 2 days before amputation and 4 days after amputation (see Figure 3B). These data

indicate that osteoblast ablation during regeneration slows the process. Data are mean ± SEM from 15 animals each. ***p < 0.001, Student's t-test.

(B, C) Images of 8 dpa *osx:NTR; osc:EGFP* fin regenerates treated with Mtz at 2 days before amputation (B) or at 4 dpa (C). Post-amputation treatment slows regeneration. *osx:*NTR fluorescence is strong in the 8 dpa regenerate from the post-amputation Mtz group, but not yet detectable in the uninjured portions proximal to the amputation plane (bracket in (C)). Arrowheads indicate amputation plane. Scale bar = 100 µm.

(D) Lengths of regenerates at 30 dpa from different treatment regimens are similar, indicating that pre- or post-amputation ablation of osteoblasts does not alter the correct recovery of proximodistal length. Data are mean ± SEM from 15 animals each.

(E, F) Longitudinal sections of 2, 3, and 4 dpa fin regenerates indicating *runx2a* (E) and *osx* (F) mRNA expression. *runx2a* and *osx* is detected both proximal and distal to the amputation plane (dotted lines) in *osx:NTR* fish treated with vehicle prior to amputation (left panels for each marker in E, F). By contrast, after treatment with Mtz to ablate osteoblasts prior to amputation (right panels), *runx2a* and *osx* are robust in the regenerate but undetectable in tissue proximal to the amputation plane. Additionally, *osx* expression is detected in intraray fibroblasts at 3 dpa regenerates of fins that had been depleted of osteoblasts prior to amputation (red bracket). Scale bar = 100 µm.

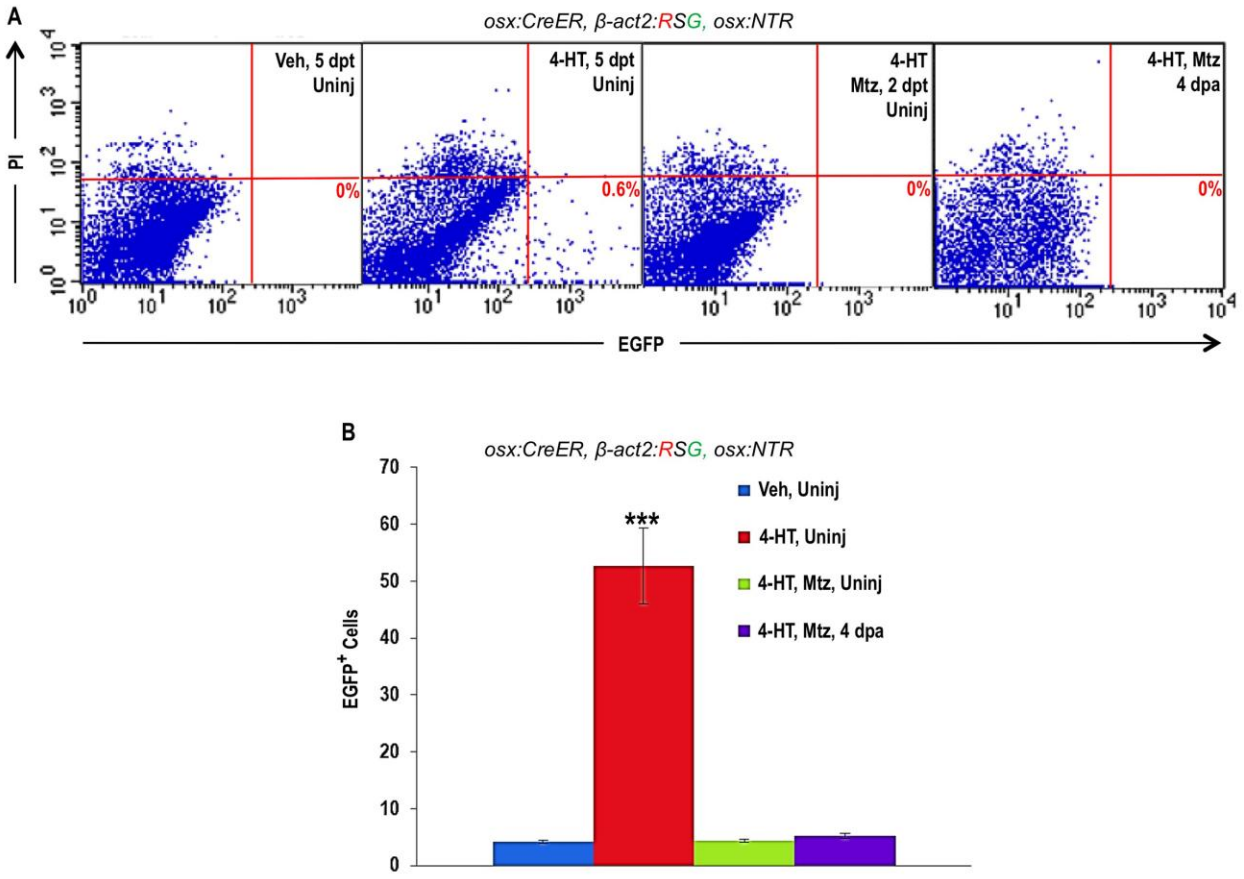

Figure S4. Loss of *β-actin2*-Driven EGFP Label after Osteoblast Ablation

(A) Flow cytometric analysis of caudal fin tissues of ***osx:CreER; β-act2:RSG; osx:NTR*** fish to detect cells expressing EGFP after 4-HT treatment. (Left panels) Fish were treated with either vehicle (left) or 4-HT (left center) and analyzed 5 days post-treatment (dpt). (Right center) An additional group of 4-HT treated fish was bathed in Mtz for 24 hours and analyzed 2 days post-Mtz treatment (dpt). (Right) A last group of 4-HT treated fish was bathed in Mtz for 24 hours, amputated and analyzed at 4 days post-amputation (dpa). Single cell suspensions were stained with propidium iodide (PI) and analyzed for EGFP. Representative plots are shown, with numbers in the lower right box indicating relative percentages of $EGFP^+$ cells.

(B) Absolute $EGFP^+$ cell counts (per 10,000 cells) from data in (A). Data are mean ± SEM from 9 animals each. ***$p < 0.001$, Student's t-test. Many cells were labeled by 4-HT in these experiments. However, fin samples from 4-HT-labeled animals treated with Mtz show no significant difference in $EGFP^+$ cell numbers from fin samples of vehicle-treated animals. Thus, Mtz treatment effectively depleted cells in the uninjured fin that had been labeled with *β-actin2*-driven EGFP fluorescence through *osx:CreER*, and these cells did not reappear in the regenerate after amputation.

Supplemental Reference

Wang, J., Panakova, D., Kikuchi, K., Holdway, J.E., Gemberling, M., Burris, J.S., Singh, S.P., Dickson, A.L., Lin, Y.F., Sabeh, M.K.*, et al.* (2011). The regenerative capacity of zebrafish reverses cardiac failure caused by genetic cardiomyocyte depletion. Development *138*, 3421-3430.